Astrophysical sources of high energy neutrinos

E. Waxman[a]WIS]Physics Faculty, Weizmann Institute of Science, Rehovot 76100, Israel
waxman@wicc.wiezmann.ac.il *

[a][

Several high energy, > 100 GeV, neutrino telescopes are currently operating or under construction. Their main motivation is the extension of the horizon of neutrino astronomy to cosmological scales. We show that general, model independent, arguments imply that ~ 1 Gton detectors are required to detect cosmic high energy neutrino sources. Predictions of models of some of the leading candidate sources, gamma-ray bursts and micro-quasars, are discussed, and the question of what can be learned from neutrino observations is addressed.

1. Introduction and summary

High energy, $>$ 100 GeV, neutrino telescopes are currently operating in deep lake water (BAIKAL, http://baikal-neutrino.da.ru/) and under Antarctic ice (AMANDA, http://amanda.berkeley.edu/amanda/). Two under-water detectors are currently under construction in the Mediterranean (ANTARES, http://antares.in2p3.fr/; NESTOR, http://www.cc.uoa.gr/ nestor/), aiming at achieving effective volumes $\sim 0.1\mathrm{km}^3$, comparable to that of AMANDA. Much larger, $\simeq 1\mathrm{km}^3$ telescopes are under construction in Antarctic ice (the IceCube extension of AMANDA, http://icecube.wisc.edu/), and under development in the Mediterranean (NEMO, http://nemoweb.lns.infn.it/). For a detailed review of the experiments, and also of their scientific goals, see [1].

The driving motivation for the construction of km-scale neutrino telescopes is the observation of cosmic point sources. At present, several neutrino telescopes monitor solar MeV neutrinos [2], and may also detect MeV neutrinos from supernova explosions, such as supernova 1987A, in our local galactic neighborhood. The construction of high-energy neutrino telescopes is aimed at extending the distances accessible to neutrino astronomy to cosmological scales. This new window onto the cosmos will provide a probe of the most powerful sources in the universe through observations of high-energy neutrinos.

The existence of extra-Galactic high energy neutrino sources is implied by the observations of ultra-high energy (UHE), $> 10^{19}$ eV, cosmic-rays. The cosmic-ray spectrum flattens at $\sim 10^{19}$ eV [3,4]. There are indications that the spectral change is correlated with a change in composition, from heavy to light nuclei [3,5]. These characteristics, which are supported by analysis of Fly's Eye, AGASA and HiRes-MIA data, and for which some evidence existed in previous experiments [6], suggest that the cosmic ray flux is dominated at energies $< 10^{19}$ eV by a Galactic component of heavy nuclei, and at UHE by an extra-Galactic source of protons. Also, both the AGASA and Fly's Eye experiments report an enhancement of the cosmic-ray flux near the Galactic disk at energies $\leq 10^{18.5}$ eV, but not at higher energies [7].

Irrespective of the nature of the cosmic-ray sources, some fraction of these particles will produce pions as they escape from the acceleration site, either through hadronic collisions with ambient gas or through interaction with ambient photons, leading to electron and muon neutrino production from the decay of charged pions.

In § 2 we discuss the upper bound implied by UHE cosmic-ray observations on the diffuse high energy neutrino flux. In § 3 we show that general, model independent arguments im-

*To appear in Nuclear Physics B (Proceedings Supplement), Proc. XXth International Conference on Neutrino Physics and Astrophysics (Munich 2002)

ply that detectors with masses equal to or larger than 1 Gton, equivalent to 1 km^3 of water, should be constructed in order to detect the expected neutrino signal in the energy range of 1 to 10^3 TeV. This conclusion applies both for the detection of point sources and for the detection of diffuse extra-Galactic flux. Even larger detectors may be required at higher energies. The construction of detectors with effective volume $\gg$ 1 km^3 at energies $\gg 10^3$ TeV may require the use of techniques different than the underwater/ice optical Cerenkov technique employed by the AMANDA, ANTARES, Baikal, IceCube, NEMO, and NESTOR experiments. Such alternative technique may be, e.g., the detection of coherent radio emission from $> 10^{16}$ eV neutrino induced cascades [8].

The origin of UHE cosmic-rays is one of the most exciting open questions of high energy astrophysics [9]. The extreme energy of the highest energy events poses a challenge to models of particle acceleration. Very few known astrophysical objects have characteristics indicating that they may allow acceleration of particles to the observed high energies. The detection of high energy neutrinos may resolve the puzzle of UHE cosmic-ray origin, as the high energy neutrinos, unlike the charged cosmic-ray protons which are subject to deflection by magnetic fields, will point directly to their sources.

The most powerful known extra-galactic objects, gamma-ray bursts (GRBs) and active galactic nuclei (AGN), are candidate sources for the production of UHE cosmic-rays, and are therefore likely sources of neutrinos in the energy range of 1 to 10^3 TeV. GRBs are transient flashes of $\sim$ 1 MeV gamma-rays lasting typically for 1 to 100 s, that are observed from sources at cosmological distances. The apparent isotropic luminosity of GRBs is $\sim 10^{52}$ erg/s. They are believed to be powered by the rapid accretion of a fraction of a solar mass of matter onto a newly born solar-mass black hole. AGN are persistent sources with apparent luminosity reaching $\sim 10^{48}$ erg/s. They are thought to be powered by mass accretion onto 10^6–10^9 solar-mass black holes, that reside at the centers of galaxies. In both GRBs and AGN, mass accretion is believed to drive a relativistic plasma outflow that results in the acceleration of high-energy particles, which emit non-thermal radiation. A similar process could also power Galactic micro-quasars, which may be considered as a scaled-down version of AGN, powered by stellar-mass black holes or neutron stars.

Despite the overall success of models in explaining the observed phenomena associated with these high energy sources, the models are largely phenomenological and our understanding of underlying physical processes is still incomplete. In all cases, neutrino observations will provide unique information on the physics of the underlying engine.

In § 4 we discuss neutrino emission from GRBs. We describe the underlying model and its predictions for neutrino telescopes, and address the question of what can be learned from neutrino observations. The discussion illustrates how neutrino observations will help resolving open questions related to the physics that underlies models of high energy astrophysical sources. In § 5 we briefly review neutrino emission from micro-quasars.

Finally, it should be emphasized that a detection of even a handful of neutrino events correlated with GRBs will allow to test for neutrino properties, e.g. flavor oscillation and coupling to gravity, and to place constraints on deviation from Lorentz invariance with accuracy many orders of magnitude better than currently possible. We discuss this in some more detail in § 4.6.

2. An upper bound to the diffuse neutrino flux

We first derive in § 2.1 the rate of generation of UHE protons implied by cosmic-ray observations. We then derive in § 2.2 the upper bound on the diffuse neutrino flux.

2.1. The UHE cosmic-ray generation rate

Fly's Eye stereo spectrum is well fitted in the energy range $10^{17.6}$ eV to $10^{19.6}$ eV by a sum of two power laws: A steeper component, with differential number spectrum $J \propto E^{-3.50}$, dominating at lower energy, and a shallower component, $J \propto E^{-2.61}$, dominating at higher energy,

$E > 10^{19}$ eV. The data are consistent with the steeper component being composed of heavy nuclei primaries, and the lighter one being composed of proton primaries. The observed UHE cosmic-ray flux and spectrum may be accounted for by a two component, Galactic + extra-Galactic model [10]. For the Galactic component, this model adopts the Fly's Eye fit,

$$\frac{dn}{dE} \propto E^{-3.50}. \quad (1)$$

The extra-Galactic proton component is derived in this model by assuming that extra-galactic protons in the energy range of 10^{19} eV to 10^{21} eV are produced by cosmologically-distributed sources at a rate

$$\dot{\varepsilon}^{\rm CR} \approx 3 \times 10^{44} {\rm erg\ Mpc^{-3}\ yr^{-1}}, \quad (2)$$

with a power law differential energy spectrum

$$\frac{dn_p}{dE_p} \propto E_p^{-n}, \quad n \approx 2. \quad (3)$$

The corresponding energy per logarithmic decade of protons is

$$E_p^2 \frac{d\dot{n}_p^{\rm CR}}{dE_p} \approx 0.7 \times 10^{44} {\rm erg\ Mpc^{-3}\ yr^{-1}}. \quad (4)$$

The spectral index, $n \approx 2$, is that expected for acceleration in sub-relativistic collisionless shocks in general, and in particular for the GRB model discussed in § 4.1. The energy generation rate, Eq. 2, is motivated by the GRB energy generation rate, compare Eq. 4 with Eq. 14.

Figure 1 compares the model prediction with the data from the AGASA [4], Fly's Eye [3], Hires [11], and Yakutsk [12] cosmic ray experiments[2]. The absolute flux measured at 10^{19} eV differs between the various experiments, corresponding to a systematic $\simeq 11\%$ ($\simeq 19\%$, $\simeq -7.5\%$) over-estimate of event energies in the AGASA (Yakutsk, HiRes) experiments compared to the Fly's Eye experiment (see also [14,10]).

[2]The Haverah Park data have recently been re-analyzed using modern numerical simulations of air-shower development [13]. The reanalysis resulted in significant changes of inferred cosmic-ray energies compared to previously published results ([6] and references quoted therein). This improved analysis is available only at energies $< 10^{19}$ eV.

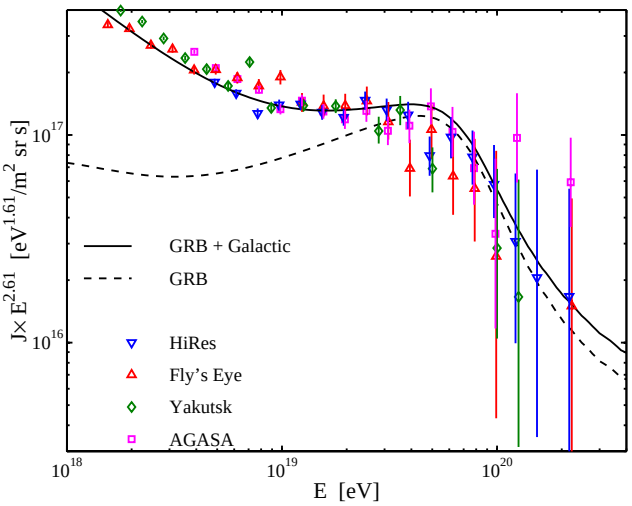

Figure 1. Model versus data. The solid curve shows the energy spectrum derived from the two-component model discussed in Section 2.1. The dashed curve shows the extra-Galactic proton contribution, Eq. 4.

These systematic shifts are well within the systematic uncertainties quoted by the experiments. We have therefore applied the appropriate small systematic shifts in absolute energy, to bring the various experiments into agreement. The results are not sensitive to the choice of absolute energy scale [10].

The choice of cosmological model is unimportant for cosmic ray energies above 10^{19} eV, which is the region of interest here. For definitness, a flat universe with $\Omega_m = 0.3$ and $\Omega_\Lambda = 0.7$, and Hubble constant $H_0 = 65\,{\rm km/s\,Mpc}$ was assumed in Fig. 1. Also, Eq. 2 represents the local, $z = 0$, energy generation rate. Motivated by the evidence for association of GRBs with star formation, it was assumed that the generation rate evolves with redshift z like $f(z) = (1+z)^3$ at low redshift, $z < 1.9$, $f(z) = {\rm Const.}$ for $1.9 < z < 2.7$, and an exponential decay at $z > 2.7$ [15].

The model described above is similar to that proposed in [16]. The improved constraints on UHECR spectrum and flux provided by the re-

cent observations of HiRes introduce only a small change, compared to [16], to the inferred energy generation rate, given by Eq. 2.

The suppression of model flux above $10^{19.7}$ eV is due to energy loss of high energy protons in interaction with the microwave background, i.e. to the "GZK cutoff" [17]. The spectra measured by Fly's Eye, HiRes and Yakutsk are consistent with the model, and hence with the existence of a GZK cutoff.

The data from the AGASA experiment, the exposure of which is $\sim 1/3$ of the combined exposure of the other experiments, is consistent with the model, and with the other experiments, up to 10^{20} eV, but show an excess of events above 10^{20} eV. The origin of this discrepancy is not yet clear. However, it should be pointed out that since the $> 10^{20}$eV flux is dominated by sources at distances ≤ 50 Mpc, over which the distribution of known astrophysical systems (e.g. galaxies, clusters of galaxies) is inhomogeneous, significant deviations from model predictions presented in Fig. 1 for a uniform source distribution are expected at this energy [16]. Clustering of cosmic-ray sources leads to a standard deviation, σ, in the expected number, N, of events above 10^{20} eV, given by $\sigma/N = 0.9(d_0/10\mathrm{Mpc})^{0.9}$ [18], where d_0 is the unknown scale length of the source correlation function and $d_0 \sim 10$ Mpc for field galaxies.

2.2. The flux bound

The energy generation rate given by Eq. 4 sets an upper limit to the neutrino flux that may be produced by sources which, like GRBs and the observed jets of AGN, are optically thin to pion producing interactions of protons with source photons (or ambient nucleons) [19].

If the high-energy protons produced by the extra-galactic sources lose a fraction $\epsilon < 1$ of their energy through production of pions before escaping the source, the resulting present-day energy density of muon neutrinos is $E_\nu^2 dN_\nu/dE_\nu \approx 0.25\epsilon t_H E_p^2 d\dot{n}_p/dE_p$, where $t_H \approx 10^{10}$yr is the Hubble time. For energy independent ϵ, the neutrino spectrum follows the proton generation spectrum, since the fraction of the proton energy carried by a neutrino produced through a photo-meson interaction, $E_\nu \approx 0.05 E_p$, is independent of the proton energy. The 0.25 factor arises because neutral pions, which do not produce neutrinos, are produced with roughly equal probability with charged pions, and because in the decay of charged pions muon neutrinos carry approximately half the charged pion energy. Thus, an upper limit to the muon neutrino flux (ν_μ and $\bar{\nu}_\mu$ combined) is obtained for $\epsilon = 1$ [19],

$$E_\nu^2 \Phi_\nu \leq E_\nu^2 \Phi_\nu^{\mathrm{WB}} \approx 0.25 \xi_Z t_H \frac{c}{4\pi} E_p^2 \frac{d\dot{n}_p^{\mathrm{CR}}}{dE_p} \approx 1.5 \times 10^{-8} \xi_Z \frac{\mathrm{GeV}}{\mathrm{cm}^2\,\mathrm{s}\,\mathrm{sr}}\,. \quad (5)$$

In the derivation of Eq. 5 we have neglected the redshift energy loss of neutrinos produced at cosmic time $t < t_H$, and implicitly assumed that the cosmic-ray generation rate per unit (comoving) volume is independent of cosmic time. The quantity ξ_Z in Eq. 5 has been introduce to describe corrections due to redshift evolution and energy loss. Assuming that the UHE proton, and hence neutrino, energy generation rate evolves rapidly with redshift, following the evolution of star formation rate [15], see § 2.1, we find that $\xi_Z \approx 3$ (with weak dependence on cosmology). The correction is small despite the strong evolution with redshift, since the universe spends only a small fraction of its present age at high z. For no evolution, we have $\xi_Z \approx 0.6 < 1$ (with weak dependence on cosmology) due to redshift energy loss of neutrinos.

There are two speculative types of sources for which the Waxman-Bahcall bound, Eq. 5, does not apply. These sources, for which we have no observational evidence to date, could in principle produce a neutrino flux exceeding the Waxman-Bahcall limit. The first special type of source is one in which neutrinos are produced by processes other than photo-meson or proton-nucleon interactions. Such sources include, e.g., decays of topological defects or of supermassive dark matter particles (see, e.g., [9]). The second type of special source is one for which the optical depth for photo-production of mesons (or for proton-nucleon interaction) is high. Examples of such optically thick scenarios include neutrinos produced in the cores of AGNs (rather than in the jets), or in a collapsing galactic nucleus [20].

3. Phenomenological considerations: km^3-scale detectors

3.1. Detection of point sources

One may obtain an estimate for the required telescope size by considering the minimal flux of a source that may be detected by a neutrino telescope of effective area A (in the plane perpendicular to the source direction) and exposure time T. The probability that a muon, produced by interaction of a muon neutrino with a nucleon, will cross the detector is given by the ratio of the muon and neutrino mean free paths, which (for water, ice) is approximately given by $P_{\mu\nu} = 10^{-4}(E_\nu/100\,\mathrm{TeV})^\alpha$, with $\alpha = 1$ for $E_\nu < 100$ TeV and $\alpha = 0.5$ for $E_\nu > 100$ TeV. A source of energy flux f_ν in neutrinos of energy E_ν will produce $N = (f_\nu/E_\nu)P_{\mu\nu}AT$ events in the detector. Thus, the flux required for the detection of N events is

$$f_\nu \sim 10^{-11} N \left(\frac{E_\nu}{100\,\mathrm{TeV}}\right)^{1-\alpha} \times \left(\frac{AT}{\mathrm{km^2 yr}}\right)^{-1} \frac{\mathrm{erg}}{\mathrm{cm^2 s}}. \quad (6)$$

For cosmological sources, with characteristic distance of $d \sim c/H0 \sim 4$ Gpc, the minimum luminosity of a detectable source is therefore

$$L_\nu > 10^{47} \left(\frac{E_\nu}{100\,\mathrm{TeV}}\right)^{1-\alpha} \left(\frac{AT}{\mathrm{km^2 yr}}\right)^{-1} \mathrm{erg/s}. \quad (7)$$

Objects with luminosity $\geq 10^{47}$erg/s, more than 13 orders of magnitude higher than the Solar luminosity, are very rare. The only known class of steady sources that produce such high luminosity are AGN. It is therefore clear that km-scale neutrino detectors are required for the detection of cosmological sources. This argument holds also for transient sources: The brightest known transients are GRBs, which produce luminosity $\sim 10^{52}$erg/s over ~ 100 s duration. Replacing $T = 1$ yr with $T = 100$ s in the above equation, implies a minimum luminosity $L_\nu \sim 10^{52}$erg/s.

A lower limit to the source flux is also set by the requirement that the signal would exceed the background produced by atmospheric neutrinos. The atmospheric neutrino flux is approximately given by $10^{-8.5}(E_\nu/500\,\mathrm{TeV})^{-\beta}\mathrm{GeV/cm^2 s\,sr}$, with $\beta = 1.7$ for $E_\nu < 500$ TeV and $\beta = 2$ for $E_\nu > 500$ TeV. Given that the expected angular resolution of the telescopes is approximately $\theta = 1$ degree, the source flux for which the signal constitutes a 5σ detection over the atmospheric background flux is

$$f_\nu \sim 10^{-12} \left(\frac{E_\nu}{10^{14.5}\mathrm{eV}}\right)^{-0.8} \times \frac{\theta}{1\mathrm{deg}} \left(\frac{AT}{\mathrm{km^2 yr}}\right)^{-1/2} \frac{\mathrm{erg}}{\mathrm{cm^2 s}}. \quad (8)$$

Thus, for km-scale detectors the atmospheric neutrino background does not pose more stringent constraints on source flux than those imposed by the requirement for a detectable signal (except at low energies).

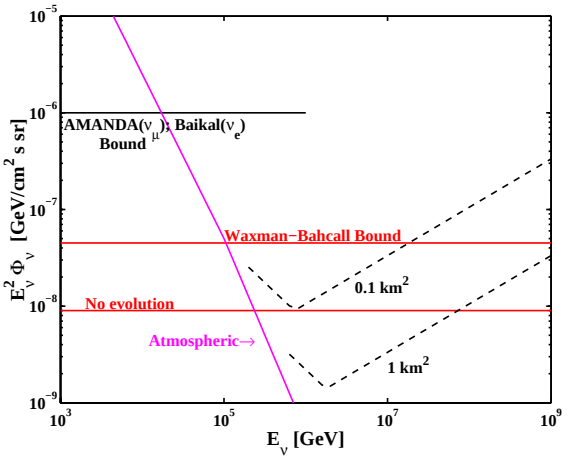

Figure 2. The projected sensitivity of km-scale detectors, based on Eqs. 9 and 10, compared with the Waxman-Bahcall upper bound on the diffuse neutrino intensity, Eq. 5. Also shown are the current experimental upper bounds imposed by the Baikal and AMANDA experiments [21], and the atmospheric neutrino background.

3.2. Detection of diffuse background

Using arguments similar to those used in § 3.1, we may obtain the minimum intensity of a diffuse neutrino background, that will allow its detection by a detector of effective area A observing 2π sr of

the sky over a duration T. The intensity required for the detection of N events is

$$E_\nu^2 \Phi_\nu \sim 10^{-9} N \quad \left(\frac{E_\nu}{100\,\mathrm{TeV}}\right)^{1-\alpha} \times \left(\frac{AT}{\mathrm{km^2 yr}}\right)^{-1} \frac{\mathrm{GeV}}{\mathrm{cm^2 s\,sr}}, \quad (9)$$

and the minimum intensity required for a 5σ detection over the atmospheric background is

$$E_\nu^2 \Phi_\nu \sim 10^{-8} \quad \left(\frac{E_\nu}{10^{14.5}\,\mathrm{eV}}\right)^{-0.8} \times \left(\frac{AT}{\mathrm{km^2 yr}}\right)^{-1/2} \frac{\mathrm{GeV}}{\mathrm{cm^2 s\,sr}}. \quad (10)$$

We compare in Figure 2 the projected sensitivity of km-scale detectors, based on Eqs. 9 and 10, with the upper bound Eq. 5 on the diffuse intensity, and with the current experimental upper bounds imposed by the Baikal and AMANDA experiments [21]. Similar to the case of point sources, km-scale detectors are required to achieve the sensitivity that may allow detection of a diffuse background. Note that, as mention in § 1, at energy $E_\nu \gg 10^3$ TeV the required effective volume is $\gg 1\mathrm{km}^3$.

4. GRBs: candidate extra-Galactic sources of > 1 TeV neutrinos

4.1. GRB model and UHE proton production

General phenomenological considerations, based on γ-ray observations, indicate that, regardless of the nature of the underlying sources, GRBs are produced by the dissipation of the kinetic energy of a relativistic expanding fireball [22]. A compact source, $r_0 \sim 10^7$ cm, produces a wind, characterized by an average luminosity $L \sim 10^{52}\mathrm{erg\ s^{-1}}$ and mass loss rate $\dot{M}$. At small radius, the wind bulk Lorentz factor, Γ, grows linearly with radius, until most of the wind energy is converted to kinetic energy and Γ saturates at $\Gamma \sim L/\dot{M}c^2 \sim 300$. Variability of the source on a time scale $\Delta t \sim 10$ ms, resulting in fluctuations in the wind bulk Lorentz factor Γ on a similar time scale, results in internal shocks in the ejecta at a radius $r \sim r_d \approx \Gamma^2 c\Delta t \gg r_0$. It is assumed that internal shocks reconvert a substantial part of the kinetic energy to internal energy, which is then radiated as γ-rays by synchrotron and inverse-Compton radiation of shock-accelerated electrons. At a later stage, the shock wave driven into the surrounding medium by the expanding fireball ejecta leads to the emission of lower-energy "afterglow."

Since the observed radiation is produced at a large distance, $\gg r_0$, from the underlying source, the model is largely independent of the nature of the underlying compact object, as long as this object is capable of producing a wind with the properties implied by observations. The underlying GRB progenitors are yet unknown. Collapse of massive stars and mergers of compact objects (e.g. of binary neutron stars) are the most widely discussed candidates [22].

The observed radiation is produced, both during the GRB and the afterglow, by synchrotron emission of shock accelerated electrons. In the region where electrons are accelerated, protons are also expected to be shock accelerated. The internal shocks within the expanding wind are mildly relativistic (in the wind rest frame), and hence we expect our understanding of non-relativistic shock acceleration to apply to the acceleration of protons in these shocks. In particular, the predicted energy distribution of accelerated protons is expected to be $dn_p/dE_p \propto E_p^{-2}$ [23], similar to the predicted electron energy spectrum, which is consistent with the observed photon spectrum.

Several constraints must be satisfied by wind parameters in order to allow proton acceleration to high energy E_p. We summarize below these constraints. The reader is referred to [24–26] for a more detailed discussion. The requirement that the acceleration time be smaller than the wind expansion time sets a lower limit to the strength of the wind magnetic field, which may be expressed as a lower limit to the ratio of magnetic field to electron energy density [24],

$$u_B/u_e > 0.02\Gamma_{2.5}^2 E_{p,20}^2 L_{\gamma,52}^{-1}, \quad (11)$$

where $E_p = 10^{20} E_{p,20}$ eV, $\Gamma = 10^{2.5}\Gamma_{2.5}$ and $L_\gamma = 10^{52} L_{\gamma,52}\mathrm{erg/s}$ is the wind γ-ray luminosity. A second constraint is imposed by the requirement that the proton acceleration time be

smaller than the proton energy loss time, which is dominated by synchrotron emission. This sets an upper limit to the magnetic field strength, which in turn sets a lower limit to Γ [24]

$$\Gamma > 130 E_{p,20}^{3/4} \Delta t_{-2}^{-1/4}. \quad (12)$$

Here, $\Delta t = 10^{-2}\Delta t_{-2}$ s. As explained in [24], the constraints Eq. 11 and Eq. 12 hold regardless of whether the fireball is a sphere or a narrow jet (as long as the jet opening angle is $> 1/\Gamma$). The luminosity in Eq. 11 is the "isotropic equivalent luminosity", i.e. the luminosity under the assumption of isotropic emission.

Internal shocks within the wind occur over a wide range of radii, corresponding to a wide range of variability time scales: $\Delta t \sim 1$ ms, the dynamical time of the source, to $\Delta t \sim 1$ s, the wind duration. Protons are therefore accelerated to high energy over a wide range of radii. In particular, at large radii the external medium affects fireball evolution, and a "reverse shock" is driven backward into the fireball ejecta and decelerates it, due to the interaction with the surrounding medium. This shock is also mildly relativistic, and its parameters are similar to those of an internal shock with $\Delta t \sim 10$ s. Protons may therefore be accelerated to ultra-high energy in this shock as well [27,25].

The constraints Eq. 11 and Eq. 12 are remarkably similar to those inferred from γ-ray observations: $\Gamma > 300$ is implied by the γ-ray spectrum in order to avoid high pair-production optical depth, magnetic field close to equipartition, $u_B/u_e \sim 0.1$, is required in order to account for both γ-ray emission and afterglow observations [22]. This suggests that GRBs and UHE s may originate from common sources.

The suggested association between GRBs and the sources of UHE protons is further strengthened by comparing the proton energy generation rate, Eq. 2, with the GRB energy generation rate. The evidence for association of GRB sources with star-formation [22], suggests that the GRB rate evolves with redshift following the star-formation rate. Under this assumption, the local ($z = 0$) GRB rate is $\approx 5 \times 10^{-10}\mathrm{Mpc}^{-3}$ yr^{-1} [28] and their average 0.1 MeV to 2 MeV γ-ray energy release is $\approx 2.5 \times 10^{53}$ erg [29], corresponding to an energy generation rate of[3]

$$\dot{\varepsilon}_\gamma^{\rm GRB} \approx 1.3 \times 10^{44} \mathrm{erg\ Mpc}^{-3}\ \mathrm{yr}^{-1}. \quad (13)$$

This rate is remarkably similar to the energy generation rate of UHE protons inferred from cosmic-ray observations, Eq. 2. Note, that although the proton generation rate, Eq. 2, is approximately twice the GRB γ-ray generation rate, Eq. 13, the corresponding energy per logarithmic decade of electrons implied by Eq. 13,

$$E_e^2 \frac{d\dot{n}_e^{\rm GRB}}{d\varepsilon_e} \approx 10^{44} \mathrm{erg\ Mpc}^{-3}\ \mathrm{yr}^{-1}. \quad (14)$$

is similar to Eq. 4. Thus, GRBs may be the sources of observed UHE cosmic-rays, provided they produce similar energy in MeV γ-rays, or, equivalently in high energy electrons, and in high energy protons.

4.2. ~ 100 TeV neutrinos

Protons accelerated in the fireball to high energy lose energy through photo-meson interaction with fireball photons. The decay of charged pions produced in this interaction results in the production of high energy neutrinos. The key relation is between the observed photon energy, E_γ, and the accelerated proton's energy, E_p, at the threshold of the Δ-resonance. In the observer frame,

$$E_\gamma\, E_p = 0.2\,\mathrm{GeV}^2\,\Gamma^2\,. \quad (15)$$

For $\Gamma \approx 300$ and $E_\gamma = 1$ MeV, we see that characteristic proton energies $\sim 10^{16}$ eV are required to produce pions. Since neutrinos produced by pion decay typically carry 5% of the proton energy, production of $\sim 10^{14}$ eV neutrinos is expected [30,19].

The fraction of energy lost by protons to pions, f_π is [30,31,25]

$$f_\pi(\epsilon_p) \approx 0.2 L_{\gamma,52}^{1/3} \Delta t_{-2}^{-1/3}. \quad (16)$$

[3]The quoted GRB rate density and γ-ray energy assume that the GRB emission is isotropic. If emission is confined to a solid angle $\Delta\Omega < 4\pi$, then the GRB rate is increased by a factor $(\Delta\Omega/4\pi)^{-1}$ and the GRB energy is decreased by the same factor. However, their product, the energy generation rate, is independent of the solid angle of emission. It is currently believed that GRB's are beamed on average into a solid angle of $4\pi/500$ [29], which implies a rate higher (total energy lower) by a factor of 500 compared to values inferred assuming isotropic emission.

Assuming that GRBs generate similar energy in high-energy protons and electrons, accounting therefore for the observed UHE cosmic-ray flux, then using Eq. 5, the expected GRB muon-neutrino flux is

$$E_\nu^2\Phi_\nu \approx 0.2\frac{f_\pi}{0.2}E_\nu^2\Phi_\nu^{\rm WB} \approx 0.9\times10^{-8}\frac{f_\pi}{0.2}{\rm GeV\,cm^{-2}s^{-1}sr^{-1}}. \quad (17)$$

This neutrino spectrum extends to $\sim 10^{16}$ eV, and suppressed at higher energy due to energy loss of pions and muons. Comparing Eq. 17 with Eq. 10, we find that ~ 20 neutrino-induced muon events per year are expected (over 4π sr) in a cubic-km detector. Note, that GRB neutrino events are correlated both in time and in direction with gamma-rays, and hence there detection is practically background free [30].

4.3. $\sim 10^{17}$ eV "Afterglow" neutrinos

High energy neutrino emission may also result from photo-meson interactions of protons accelerated to high energies in the reverse shocks driven into the fireball ejecta at the initial stage of interaction of the fireball with its surrounding gas, which occurs on time scale $T \sim 10$ s (see § 4.1). Optical–UV photons are radiated by electrons accelerated in shocks propagating backward into the ejecta. The interaction of these low energy, 10 eV–1 keV, photons and high energy protons produces a burst of duration $\sim T$ of ultra-high energy, 10^{17}–10^{19} eV, neutrinos, as indicated by Eq. 15 [27].

The expected muon neutrino intensity depends on the density of the surrounding medium [27,32], which may differ by orders of magnitude between models assuming different GRB progenitors. If GRB fireballs expand into typical density interstellar medium, $n \sim 1{\rm cm^{-3}}$, as expected if the GRBs are the result of mergers of compact objects, the expected intensity is

$$E_\nu^2\Phi_\nu \approx 10^{-10}\left(\frac{E_\nu}{10^{17}{\rm eV}}\right)^\beta {\rm GeV\,cm^{-2}s^{-1}sr^{-1}}, \quad (18)$$

with $\beta = 1/2$ for $E_\nu > 10^{17}$eV and $\beta = 1$ otherwise. If GRB fireballs expand into massive stellar winds ($n \sim 10^4{\rm cm^{-3}}$), as expected if GRBs result from the collapse of massive stars, then

$$E_\nu^2\Phi_\nu \approx 10^{-8}\,\min\{1, E_\nu/10^{17}{\rm eV}\}\frac{\rm GeV}{\rm cm^{-2}s\,sr}. \quad (19)$$

The neutrino flux is expected to be strongly suppressed at energy $E_\nu > 10^{19}$ eV, since protons are not expected to be accelerated to energy $E_p \gg 10^{20}$ eV.

4.4. ~ 5 TeV "Collapsar" neutrinos

Lower energy, ~ 5 TeV, neutrino emission may be expected in the case where GRBs originate from the collapse of massive stars [33]. In this scenario, accretion onto a black hole, produced by the collapse of the massive star (the "collapsar") core, drives a relativistic jet that propagates through the stellar envelope along the collapsar rotation axis. The shocks producing the γ-rays must occur after the fireball has emerged from the stellar envelope. While the jet is making its way out of the star, its rate of advance is slowed down in a termination shock that heats the stellar plasma to keV temperatures, and additional internal shocks are expected in the pre-deceleration interior jet. The latter can accelerate protons to $> 10^5$ GeV, which interact with the X-ray photons in the stellar jet cavity leading to pion production and hence electron and muon neutrinos (and anti neutrinos) with energies $E_\nu \geq 5$ TeV. These neutrinos appear as a precursor signal, lasting for time scales of tens of seconds prior to the observation of any γ-rays produced outside the star by a collapsar-induced GRB. The TeV neutrino fluence from an individual collapse at cosmological distance $z \sim 1$ implies ~ 0.1 upward moving muons per collapse in a 1 km^3 detector.

4.5. Implications: GRB models

The emission of $\sim$ 100 TeV neutrinos discussed in § 4.2 is independent of the underlying GRB progenitor. It is a natural outcome of the "generic" fireball model described in § 4.1, where the observed γ-rays are produced by internal shocks within a dissipative relativistic wind. The major underlying assumption, upon which the predictions depend, is that the fireball momentum is carried (after the initial stage of acceleration) by relativistic protons. The predicted flux, Eq. 17, implies ~ 20 neutrino-induced muon

events per year in a cubic-km detector. Neutrino telescopes may therefore allow to test underlying assumptions of the fireball model. Detection of the predicted signal will also provide strong support for the model of UHE cosmic-ray production in GRBs.

The emission of $\sim 10^{17}$ eV neutrinos, § 4.3, is also a natural prediction of the fireball model. The expected neutrino intensity depends strongly, however, on the GRB progenitor, compare Eqs. 18 and 19. Detection of such UHE neutrinos may therefore provide constraints on the progenitor type.

Finally, emission of ~ 5 TeV "collapsar" neutrinos is expected only for collapsar GRB progenitors. The detection of a ~ 5 TeV neutrino precursor will therefore provide a clear signature of the collapsar model.

4.6. Implications: Lorentz invariance, The weak equivalence principle, and neutrino oscillations

Detection of neutrinos from GRBs could be used to test the simultaneity of neutrino and photon arrival to an accuracy of ~ 1 s (~ 1 ms for short bursts), checking the assumption of special relativity that photons and neutrinos have the same limiting speed [30]. These observations would also test the weak equivalence principle, according to which photons and neutrinos should suffer the same time delay as they pass through a gravitational potential. With 1 s accuracy, a burst at a distance of 1 Gpc would reveal a fractional difference in limiting speed $\sim 10^{-17}$, and a fractional difference in gravitational time delay of order 10^{-6} (considering the Galactic potential alone). Previous applications of these ideas to supernova 1987A, where simultaneity could be checked only to an accuracy of order several hours, yielded much weaker upper limits: of order 10^{-8} and 10^{-2} for fractional differences in the limiting speed and time delay, respectively.

The model discussed above predicts the production of high energy muon and electron neutrinos with a 2:1 ratio (tau neutrinos may be produced by photo-production of charmed mesons; however, the higher energy threshold and lower cross-section for charmed-meson production, compared to pion production, typically imply that the ratio of charmed-meson to pion production is 10^{-4} [30]). Because of neutrino oscillations, neutrinos that get here are expected to be almost equally distributed between flavors for which the mixing is strong. Upgoing taus, rather than muons, would be a distinctive signature of such oscillations. It may be possible to distinguish between taus and muons in a km^3-scale detector, since at 10^3 TeV the tau decay length is ~ 1 km. This will allow a "tau appearance experiment".

5. Micro-quasars: Galactic candidate sources

The jets associated with Galactic micro-quasars [34] are believed to be ejected by accreting stellar-mass black holes or neutron stars. Much like for AGN, the content of the jets is an open issue. The dominant energy carrier in the jet is at present unknown (with the exception of the jet in SS433). Scenarios whereby energy extraction is associated with spin-down of a Kerr (rotating) black hole favor electron-positron composition (although baryon admixture is an issue), while scenarios in which an initial rise of the X-ray flux leads to ejection of the inner part of the accretion disk imply electron-positron jets, as widely claimed to be suggested by the anti-correlation between the X-ray and radio flares seen during major ejection events. A possible diagnostic of electron-positron jets is the presence of Doppler-shifted spectral lines, such as the Hα lines as seen in SS433. The detection of such lines from jets having a Lorentz-Γ factor well in excess of unity (as is the case in the super-luminal micro-quasars) may, however, be far more difficult than in SS433, as the lines are anticipated to be very broad.

Neutrino telescopes may prove to be a much sharper diagnostic tool. If the energy content of the jets in the transient sources is dominated by electron-proton plasma, then a several hour outburst of 1 to 100 TeV neutrinos (and high-energy photons) produced by photo-production of pions should precede the radio flares associated with major ejection events [35]. Several neutrinos may be detected during a single outburst by a km^3-

scale detector [35,36], thereby providing a powerful probe of micro-quasar jet physics and of their innermost structure.

REFERENCES

1. HENAP report to PaNAGAIC, http://www.ifae.es/henap/
2. See review talks by J. N. Bahcall, G. Bellini, V. Gavrin, A. Hallin, T. Kirsten, K. Lande, S. Schönert & M. Smy, these proceedings.
3. Bird, D. J. *et al.* 1994, Astrophys. J. **424**, 491.
4. Hayashida N. *et al.* 1999, Astrophys. J. **522**, 225 and astro-ph/0008102.
5. Dawson, B. R., Meyhandan, R., and Simpson, K. M., 1998, Astropart. Phys. **9**, 331; Abu-Zayyad, T. et al. 2001, ApJ **557**, 686.
6. Watson, A. A. 1991, Nuc. Phys. B (Proc. Suppl.) **22**, 116.
7. Bird, D. J. *et al.* 1998, Astrophys. J. **511**, 739; Hayashida N. *et al.* 1999, Astropart. Phys. **10**, 303.
8. See review talks by J. Learned & A. Letessier-Selvon, these proceedings.
9. Bhattacharjee, P. & Sigl, G. 2000, Physics Reports, 327, 109; Nagano, M. & Watson, A. A. 2000, Rev. Mod. Phys. 72, 689.
10. Bahcall, J. N. & Waxman, E. 2002, submitted to Phys. Lett. B, hep-ph/0206217.
11. Abu-Zayyad, T., et al., 2002, submitted PRL, astro-ph/0208243.
12. N. N. Efimov *et al.*, in *Proceedings of the International Symposium on Astrophysical Aspects of the Most Energetic Cosmic-Rays*, edited by M. Nagano and F. Takahara (World Scientific, Singapore 1991), p. 20.
13. Hinton, J., et al., Proc. Ultra High Energy Particles from Space, Aspen 2002 (http://hep.uchicago.edu/ jah/aspen/aspen2.html).
14. Yoshida, S., *et al.*, Astropar. Phys. **3**, 151 (1995).
15. S. J. Lilly, O. Le Fevre, F. Hammer and D. Crampton, Astrophys. J. **460**, L1 (1996); P. Madau, H. C. Ferguson, M. E. Dickinson, M. Giavalisco, C. C. Steidel and A. Fruchter, Mon. Not. Roy. Astron. Soc. **283**, 1388 (1996).
16. Waxman, E. 1995, Astrophys. J. Lett. **452**, L1.
17. K. Greisen 1966, Phys. Rev. Lett. **16**, 748; Zatsepin, G. T. and Kuzmin, V. A. 1966, JETP **4**, 78.
18. Bahcall, J. N. and Waxman, E. 2000, Astrophys. J. **542**, 542.
19. Waxman, E. and Bahcall, J. N. 1999, Phys. Rev. D **59**, 023002; Bahcall, J. N. & Waxman, E. 2001, Phys. Rev. D **64**, 023002.
20. Stecker, F., Done, C., Salamon, M., and Sommers, P. 1991, Phys. Rev. Lett. **66**, 2697, erratum Phys. Rev. Lett. **69**, 2738 (1992); Berezinsky, V. S. and Dokuchaev, V. I. 2002, Nuc. Phys. B (Proceedings Supplements), **110**, 522.
21. See review talks by G. Domogatsky & D. Cowen, these proceedings.
22. For updated review see Mészáros, P. 2002, ARA&A 40, 137.
23. For review see, e.g., Blandford, R., & Eichler, D. 1987, Phys. Rep. **154**, 1.
24. Waxman, E. 1995, Phys. Rev. Lett. **75**, 386.
25. Waxman, E. in *Physics & Astrophysics of Ultra-High-Energy Cosmic Rays*, Eds. M. Lemoine & G. Sigl (Springer), Lecture Notes in Physics **576**, 122-154 (2001).
26. Waxman, E. 2002, submitted to ApJL (astro-ph/0210638).
27. Waxman, E., & Bahcall, J. N. 2000, Ap. J. **541**, 707.
28. Schmidt, M. 2001, Astrophys. J. **552**, 36.
29. Frail, D. A. *et al.* 2001, Astrophys. J. Lett. **562**, L55.
30. Waxman, E., & Bahcall, J. N. 1997, Phys. Rev. Lett. **78**, 2292.
31. Guetta, D., Spada M., & Waxman, E. 2001, Ap. J. **559**, 101.
32. Dai, Z. G., & Lu, T. 2001, Ap. J. **551**, 249.
33. Mészáros, P., & Waxman, E. 2001, Phys. Rev. Lett. **87**, 1002
34. Mirabel, I. F. & Rodriguez, L. F. 1999, ARA&A, **37**, 409.
35. Levinson, A. & Waxman, E. 2001, Phys. Rev. Lett. 87, 171101.
36. Distefano, C., Guetta, D., Waxman, E., Levinson, A. 2002, ApJ 575, 378